Mangrove vegetation assessment in the Santiago River Mouth, Mexico, by means of supervised classification using Landsat TM imagery

Article *in* Forest Ecology and Management · June 1998

DOI: 10.1016/S0378-1127(97)00289-2

CITATIONS
95

READS
480

4 authors, including:

Pedro Ramírez-García
National Autonomous University of Mexico
37 PUBLICATIONS **488** CITATIONS
SEE PROFILE

Jorge Lopez-Blanco
Instituto Nacional de Ecología y Cambio Climático INECC, México City, M…
72 PUBLICATIONS **1,982** CITATIONS
SEE PROFILE

Daniel Ocana
Comisión Nacional para el Conocimiento y Uso de la Biodiversidad
5 PUBLICATIONS **254** CITATIONS
SEE PROFILE

ELSEVIER

Forest Ecology and Management 105 (1998) 217–229

Forest Ecology and Management

Mangrove vegetation assessment in the Santiago River Mouth, Mexico, by means of supervised classification using Landsat TM imagery

Pedro Ramírez-García [a,*], Jorge López-Blanco [b,1], Daniel Ocaña [a,2]

[a] *Instituto de Biología, UNAM. Apdo. Post. 70-233, 04510 México, D.F., Mexico*
[b] *Instituto de Geografía, UNAM, Apdo. Post. 20-850, 04510 México, D.F., Mexico*

Received 4 April 1997; accepted 30 September 1997

Abstract

This paper presents a mangrove vegetation assessment from 1970 to 1993 of the Santiago River Mouth, Nayarit, West of Mexico. The aims of this work are to describe the plant composition and structure of mangrove in the study area, and to evaluate the deforestation level and its amplitude by means of a retrospective analysis of the cover and distribution area of mangrove species using a LandsatTM image, aerial photographs and oblique video. Mangrove of the study area is dominated by *Laguncularia racemosa* with the average importance value of 158.18 and 400 ha of plant cover, followed by *Avicennia germinans*, with an average importance value of 138.52 and 324 ha of plant cover. Mangrove showed seven height and five diametrical classes that include the two dominant species. *L. racemosa* was the dominant species in six of the eight compass lines. The highest absolute frequencies for both dominant species were found in the second height class frequency, and the first diametric class frequency. Cover area and distribution of mangrove in the study area were mapped using a LandsatTM5 image (April 1993). A supervised classification was applied using the maximum likelihood algorithm, considering ten initial classes. This classification was evaluated by obtaining a classification error matrix and by assessing its accuracy. The mangrove vegetation area reported before, considering the same area for image analysis, resulted to be overestimated in 56% regarding the value obtained in our photointerpretation (1065 ha). From the latter mangrove area, the current cover is 724 ha, which represents a decrease of 32% in a 23-yr period. © 1998 Elsevier Science B.V.

Keywords: Deforestation; Vegetation analysis; *Laguncularia racemosa*; *Avicennia germinans*; Remote sensing; Discriminant analysis

1. Introduction

In the last decades, the environmental and ecological roles that mangrove vegetation ecosystems play have been defined and recognized (Chapman, 1969; Blasco, 1988a,b). If we want to assess and challenge the deforestation problem on mangrove covering areas, we have to recognize that many people in coastal areas (tropics and subtropics) need to open land for grazing and farming purposes, and more recently for shrimp aquaculture production. These disturbance activities, mainly in developing countries, have been specific and direct causes on cover retraction and destruction of mangrove communities.

* Corresponding author. E-mail: armora@servidor.unam.mx.
[1] E-mail: jlblanco@servidor.unam.mx.
[2] E-mail: danielo@mail.ibiologia.unam.mx.

PII S0378-1127(97)00289-2

Furthermore, there are other indirect causes too, such as construction of roads, channels, harbors, dams, and infrastructure for tourism activities. Other causes, are natural origin phenomena as hurricanes, storms, tides, flooding, and river trajectories changes. If we consider that all those causes can be aggregated (mixed) in a specific spatial and temporal context, the mangrove ecosystem damage, in some cases, could be irreversible.

Mangroves are the most characteristic vegetation of tropical and subtropical coasts worldwide (Chapman, 1969), and in Mexico, where this vegetation covers large areas in the Pacific, Gulf of Mexico, and the Caribbean coasts (Lot and Novelo, 1990). Mangroves in the Mexican Pacific coasts comprise between 22 and 23% (170,579 ha) of the total area of Mexican mangroves (660,000 ha; Blasco, 1988a; Flores-Verdugo et al., 1992). One of the largest mangrove areas in the Mexican Pacific slope is located in the Teacapán–Agua Brava–Marismas Nacionales Lagoonal System, with 113,238 ha (Flores-Verdugo et al., 1992). This area extends toward the southeastern extreme of the lagoonal system mentioned, which includes the mangrove vegetation of the Santiago River Mouth (Río Grande de Santiago) where the study area is located.

The distribution and abundance of mangroves in different regions of the world have been assessed using a variety of techniques. Some of these have been performed using aerial panchromatic and infrared photographs (Rollet, 1974a,b,c; Everitt and Judd, 1989), satellite imagery (Blasco, 1988b, 1991; Lanza et al., 1993), and video imagery (Everitt et al., 1991).

Our main interest to perform this study consisted of applying a method of vegetation analysis to obtain a detailed characterization of plant community structure. Furthermore, both digital analysis on LandsatTM-oblique video imagery and photo-interpretation techniques were also used, in order to determine the spatial extent and change in vegetation cover, as well as to establish the regional cover and dominance of mangrove associations, and some of their dominant species. This allowed a comparison of data obtained from image analysis with those obtained by field work.

The importance of this study is to know the current state (considering information until 1993) of the mangrove community in the study area. We must taking into account that, in the near future, important changes in such community (because of streamflow regulation and decreasing of sediment yield) will be introduced caused by the starting in operation in 1994 of the Aguamilpa hydroelectric plant, which was established 70 km upstream from the Santiago River mouth. Considering that, we have evaluated the structure of the mangrove vegetation, as well as its cover change in the study area from 1970 to 1993.

The aims of this work are to describe the plant composition and structure of mangrove in the Santiago River Mouth, to evaluate the deforestation level and its extent, from both natural and anthropogenic agents, and to make a retrospective analysis of cover and distribution area of mangrove species using satellite image and aerial photographs.

2. Material and methods

2.1. Study site

The study area at the Río Santiago Mouth is located in Nayarit State, at 21°37′30″ latitude N and 105°27′30″ longitude W (Fig. 1). It has a deltaic arrangement with bar beaches, spits and beachridges. From a geomorphologic point of view it is a broad alluvial plain, in which intertidal plains predominate toward the mouth (Galavís and Gutiérrez, 1989). The study area is characterized by a subhumid warm climate with rainy summers and a thermal range of 6.5°C. Mean annual temperature is 26.6°C, with the

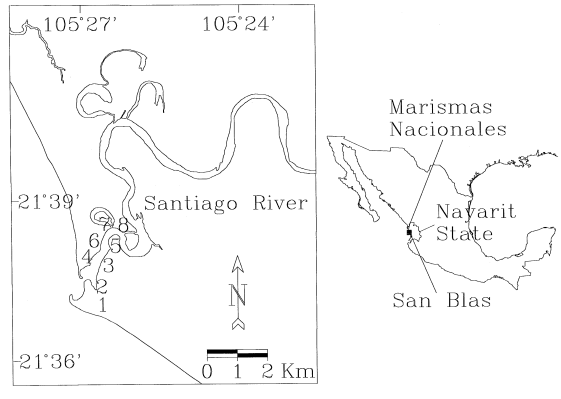

Fig. 1.

coldest months being January and February (23°C), and June the warmest (29.5°C). Total annual precipitation is 1267.4 mm, April being the driest month (3.8 mm) and August the wettest (371.6 mm; García, 1988).

The area is part of the morphotectonic subprovince of the Pacific Coastal Plains, that belongs to the Province of Plain and Northwest Sierras. Lithologic composition at the subprovince is of clastic sediments from the quaternary period with transitional rocky bodies (continental–marine), developed by the evolution of complex delta systems which prograde toward the Pacific Ocean (Ferrusquía-Villafranca, 1993).

Hydrologically, it belongs to the Lerma–Chapala–Santiago River Basin, which covers a total area of 124,520 km^2. The Santiago River is 450 km long, from its source in the Chapala Lake at 1521 m above sea level (Secretaría de Recursos Hidráulicos, 1965).

2.2. Forest structure

The study area was visited eight times, of five days each between July 1993 and June 1994. In each visit, a compass line perpendicular to the river traject was sampled (Fig. 1), each with a length of 100 m and 11 sampling stations. The point centered quadrat method was used to estimate structural parameters, tree height, diameter at breast height (DBH; the minimum sampling diameter was 2 cm), density, dominance, frequency, and importance value for each species present (Cox, 1967; Mueller-Dombois and Ellenberg, 1974; Cintrón and Scheaffer, 1984). The dominance was obtained from the product of basal area average by density per species, and the importance value was calculated adding the following relative values: density, dominance and, frequency. Using the rule of Sturges (1926), the number of intervals of frequency distribution of DBH and height classes were established.

2.3. Image processing

The cover area and zonation of the mangrove in the study area were mapped using a LandsatTM5 image (April 1993), using a supervised classification technique (Lillesand and Kiefer, 1994). A matrix of 1024×1024 with a pixel size of 25 m, of bands 1 to 5 and 7 was used. A helicopter flight was performed to obtain oblique video imagery of the study area, in order to validate the land use patterns and distribution of current vegetation, inferred from the remote sensing analysis. A subarea of 400×500 elements was then extracted, in order to study a representative area of the site. Histogram stretching was applied to each band as well as edge enhancement filtering, in order to visually enhance the information and to generate color composites that could ease the georeference procedure. The color composites used were $4/5/1$ and $3/2/1$.

The image was georeferenced considering the UTM coordinates system, using 19 control points identified in the topographic map. The sigma value in this procedure was of 0.98 pixel of root mean square error to assign coordinates. With the optimal index factor (OIF), the best band combination was defined to create a color composite (ITC, 1993). The variance–covariance matrix was calculated using six bands (1–5 and 7); principal components analysis was performed to determine the bands that explained most of the data variability. Finally, a supervised classification of the subimage was performed by the maximum likelihood algorithm, considering ten initial classes (training areas) and using the Mahalanobis distances as the clustering parameter (ITC, 1993). This classification was evaluated by obtaining a classification error matrix and by assessing its accuracy (Lillesand and Kiefer, 1994). The error matrix was obtained by the crossing GIS capability, using the raster map of the training areas, crossing to the raster map derived from the supervised classification, from this resulted a pixel value table of each map and its corresponding sum of pixels. Also, in order to test for significance differences between spectral classes obtained from supervised classification a discriminant analysis of spectral classes was performed.

2.4. Temporal and spatial analysis of vegetation

In order to estimate the surface of the mangrove in the study area, and considering the magnitude of changes in the river trajectory, the map obtained from the supervised classification was compared with the digitized map from the Land Use and Topo-

Table 1
Structural composition of mangrove sampling (compass lines)

Compass line	Total density (trees ha^{-1})	Species	Species density (trees ha^{-1})	Relative density (%)	Dominance (m^2 h^{-1})	Relative dominance (%)	Relative frequency (%)	Importance value
T1	1415	*A. germinans*	579	41	12.17	41	47	129
		L. racemosa	836	59	32.23	59	53	171
T2	1513	*A. germinans*	688	46	14.17	40	46	132
		L. racemosa	791	52	21.76	59	46	159
		R. mangle	34	2	0.46	1	6	9
T3	544	*A. germinans*	433	80	10.20	80	67	226
		L. racemosa	111	20	2.67	20	33	74
T4	1428	*A. germinans*	1072	75	14.25	60	65	199
		L. racemosa	357	25	19.40	40	35	101
T5	1154	*A. germinans*	184	16	5.94	24	35	75
		L. racemosa	970	84	17.08	76	65	225
T6	1264	*A. germinans*	259	20	0.33	23	32	76
		L. racemosa	948	75	30.38	74	58	207
		R. mangle	57	5	0.46	3	11	18
T7	1558	*A. germinans*	1169	75	34.12	77	65	217
		L. racemosa	390	25	6.46	23	35	83
T8	2978	*A. germinans*	474	15	2.95	23	35	74
		L. racemosa	2504	85	33.30	77	65	226
Average	1406.8	*A. germinans*	607.3	46.0	11.87	46.0	49.0	141.0
		L. racemosa	713.4	53.1	20.41	53.5	48.7	155.5
		R. mangle	45.5	3.5	0.46	2.0	8.5	13.5

Table 2
Principal components (PC) Matrix (eigenvectors) and percentage of variance

Components	TM 1 band	TM 2 band	TM 3 band	TM 4 band	TM 5 band	TM 7 band	% variance
1st PC	0.126	0.082	0.202	0.434	0.776	0.383	88.67
2nd PC	0.434	0.282	0.551	−0.514	−0.143	0.379	7.32
3rd PC	0.188	0.122	0.212	0.732	−0.586	0.158	3.07
4th PC	−0.293	−0.190	−0.386	−0.106	−0.182	0.827	0.57
5th PC	−0.614	−0.399	0.680	0.000	−0.035	0.000	0.20
6th PC	−0.545	0.838	0.000	0.000	0.000	0.000	0.000

graphic maps (Villa Juárez sheet, code F-13-C-28, 1:50,000 scale) edited by CETENAL (1973a,b), and by our photointerpretation of aerial photographs taken in 1970 also by CETENAL. We considered the river trajectories in the years 1970, 1990 (reported by Ortíz-Pérez and Romo-Aguilar, 1994). The river paths of 1970, 1990 and, March 1993 were digitized, integrating them to the previously digitized paths of the CETENAL map, the aerial photographs (1:25,000 scale, 1970), and the river path in the LandsatTM image (April, 1993). The segments that describe the river paths were combined in a GIS and the mangrove areas affected by the river were delineated. This process was executed using ILWIS (version 1.41) software-package, installed on a personal computer.

3. Results

3.1. Vegetation analysis

The mangrove community in the study area is composed of four species, *Avicennia germinans*, *Conocarpus erecta*, *Laguncularia racemosa*, and *Rhizophora mangle*. The dominant species are *A. germinans* and *L. racemosa*. The former has a density range of 184 to 1169 trees ha^{-1} and a dominance range of 0.33 to 34.12 m^2 ha^{-1}, whereas *L. racemosa* has a density range of 111 to 2054 trees ha^{-1} and a dominance range of 2.67 to 33.3 m^2 ha^{-1}. *R. mangle* has a minimum density of 34 and a maximum of 57 trees ha^{-1}, with a dominance value of 0.46 m^2 ha^{-1}. *C. erecta* was found infrequently only upstream, at the river banks and margins, near the agricultural lands, so its presence in the main core of the mangrove was null. The absolute importance value of the two dominant species ranges from 74 to 226 (Table 1).

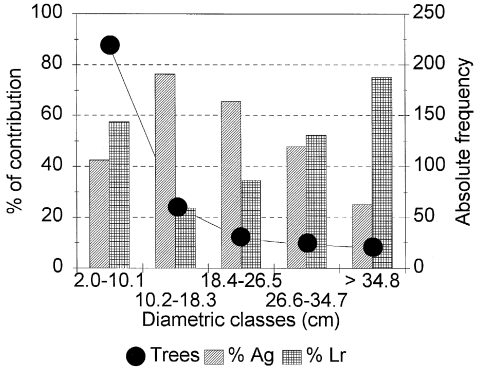

Fig. 3.

The mangrove showed seven height and five diametrical classes that include the two dominant species. The height class with the highest frequency was 4.4–6.7 m, represented by *A. germinans* trees in 42.7%, with an absolute frequency of 46 individuals, and by *L. racemosa* trees in 57.3%, with an absolute frequency of 62 individuals (total 108). The height class with the lowest absolute frequency was represented by the 14.0–16.3 m, with 50% of each of the two dominant species trees, and an absolute frequency of 11 individuals of each species (total 22; Fig. 2).

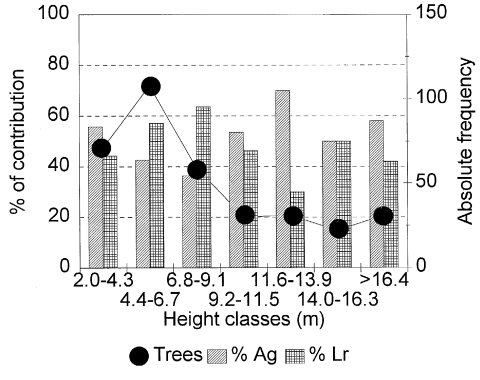

Fig. 2.

Table 3
Supervised classification using a maximum likelihood algorithm

Category	No. of pixels	% of pixels	Area (ha)
Grazing land (G)	32723	16.36	2058
Low deciduous forest (Fo)	9610	4.80	604
Water (W)	41722	20.86	2624
L. racemosa (L)	6372	3.18	400
A. germinans (AV)	5154	2.57	324
Dune vegetation (D)	9594	4.79	6
Secondary vegetation (V)	1991	0.99	125
Farming land (C)	50957	25.47	3205
Sand (S)	1683	0.84	105
Marsh (M)	2388	1.19	150
Not classified	37806	18.90	2378

The dominant diametric class with the highest frequency was that of 2.0–10.1 cm, composed of *A. germinans* in 42.5%, with an absolute frequency of 93 trees, and by *L. racemosa* in 57.5%, with an absolute frequency of 126 trees (total 219). The class with the lower frequency was represented by those

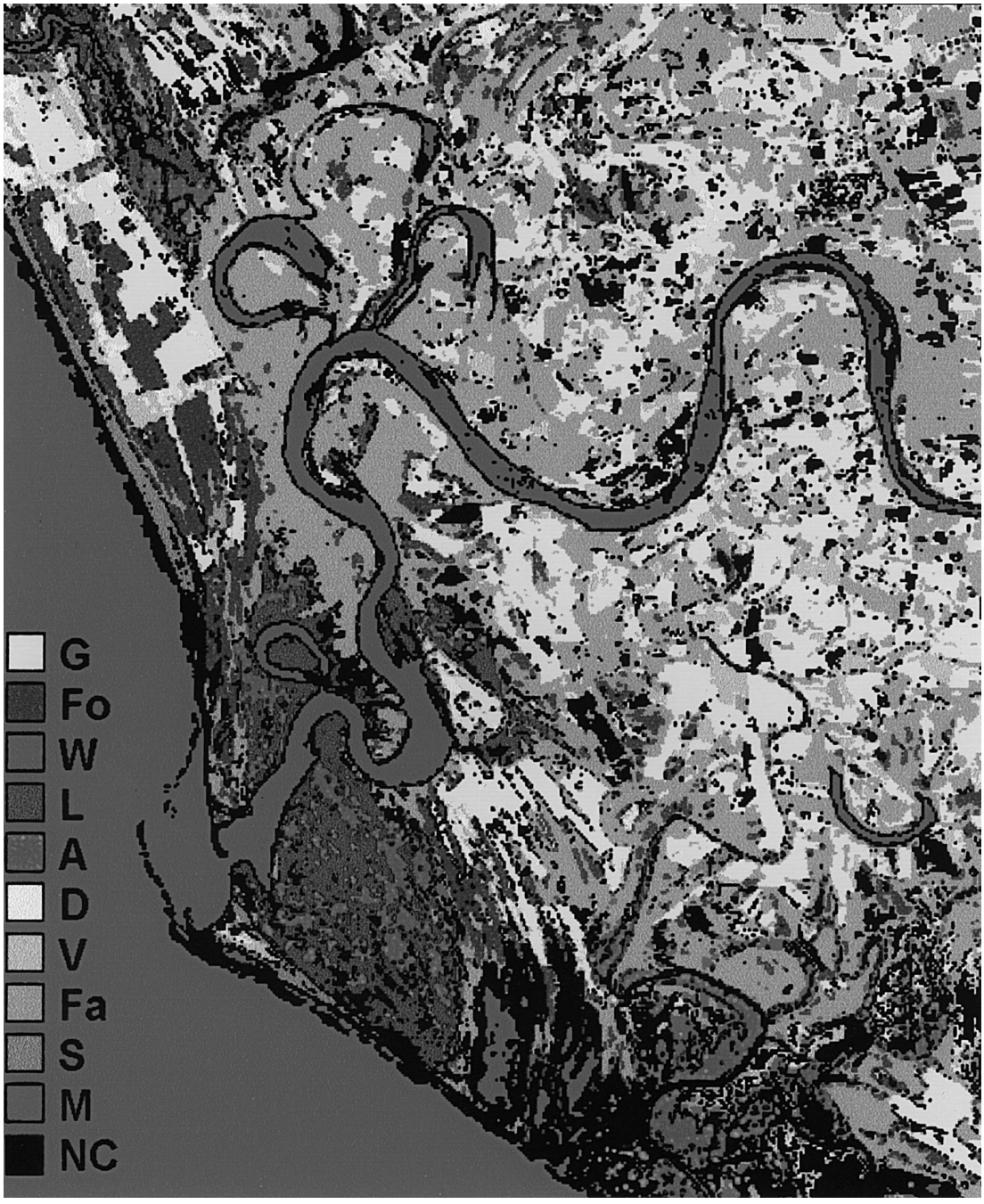

Fig. 4.

Table 4
Classification error matrix for the supervised classification

Category	G	Fo	W	L	A	D	V	Fa	S	M	Σ real + inclusion
G	1107	1						3			1111
Fo		765						2			767
W			2276								2276
L				415	18						433
A				13	526						539
D	104	7				242	1				354
V	42					15	138				195
Fa	4	70						1409		4	1487
S									64		64
M				1				1		71	73
Σ real + omission	1257	843	2276	429	544	257	139	1415	64	75	7299

G = grazing lands, Fo = low deciduous forest, W = water, L = *L. racemosa*, A = *A. germinans*, D = dune vegetation, V = secondary vegetation, Fa = farming land, S = sand, M = marsh.

trees with a DBH greater than 34.8 cm, which consisted of *A. germinans* in 25%, with an absolute frequency of 5 trees, and of *L. racemosa* in 75%, with an absolute frequency of 15 trees (total 20; Fig. 3).

L. racemosa was the dominant species in six of the eight compass line. The highest dominances were obtained in compass line 1 (T1) and 8 (T8) (Fig. 1), with 32.23 and 33.3 m^2 ha^{-1}, respectively. The highest dominance value for *A. germinans* was 34.12 m^2 ha^{-1} in compass line 7 (T7). The lowest dominance value for *L. racemosa* was observed in compass line 3 (T3), with 2.67 m^2 ha^{-1} (Table 1).

In almost every compass line where *L. racemosa* was the dominant species, its density was the greatest, for example, 2504 trees ha^{-1} in T8. Nevertheless, the situation differed for T4, since although the dominance was greater for *L. racemosa*, with 19.4 m^2 ha^{-1}, the density of *A. germinans* was greater, with 1072 trees ha^{-1}, (Table 1). On the basis of the importance value of each species (Table 1), we observed that five compass lines were dominated by the species *L. racemosa* (T1, T2, T5, T6 and T8), and three by *A. germinans* (T3, T4 and T7). *R. mangle* was an uncommon species, with densities below 57 trees ha^{-1}, a maximum dominance of 0.46 m^2 ha^{-1}, and a small importance value, between 9.4 and 18. This species was found only in compass lines T2 and T6.

The highest absolute frequencies for both dominant species were found in the second height class frequency (Fig. 2), and the first diametric class fre-

Table 5
Evaluation of the supervised classification of the subimage evaluated

Category	Producer's accuracy (%)	Omission probability (%)	User's accuracy (%)	Inclusion probability (%)
Grazing land (G)	88.1	11.9	99.6	0.4
Low deciduous forest (Fo)	90.8	9.2	99.8	0.2
Water (W)	100	0.0	100	0.0
L. racemosa (L)	96.7	3.3	95.8	4.2
A. germinans (AV)	96.7	3.3	97.6	3.4
Dune vegetation (D)	94.2	5.8	68.4	31.6
Secondary vegetation (V)	99.3	0.7	70.8	29.2
Farming land (C)	99.6	0.4	94.8	5.2
Sand (S)	100	0.0	100	0.0
Marsh (M)	94.7	5.3	97.3	2.7
Total accuracy = $((1107 + 765 + 2276 + 415 + 526 + 242 + 138 + 1409 + 64 + 71)/7299)^{*} 100 = 88.5\%$				

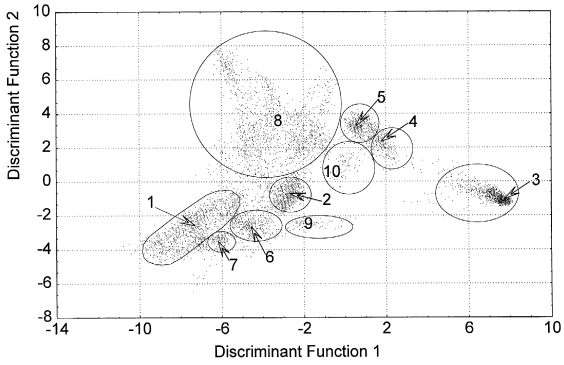

Fig. 5.

quency (Fig. 3). The mangrove community in this area was dominated by individuals with a height between 2 and 6.7 m and with a DBH between 2 and 10.1 cm. Young individuals were particularly abundant in the river borders and in the recently formed banks.

According to the physiognomical classification of mangroves (Lugo and Snedaker, 1974), the mangrove of Santiago River mouth is classified as a river mangrove toward the river bank, where *L. racemosa* dominates, and as a basin mangrove toward the internal part, which covers the entire alluvial plain, and where *A. germinans* is dominant.

3.2. Image analysis

In order to analyze, not only at local-scale level (compass lines) the mangrove community, but in a different way that clearly reflects the spatial at general-scale, that is, cover area, spatial distribution and cover changes by river dynamics trajects, we made a digital image processing using the LandsatTM image.

Principal components analysis applied to the six spectral bands showed that bands 3, 4 and 5 explained 99.06% of the total variance of the data (Table 2). First three principal components estimated using the color composite of bands 4/5/3, which comprised 7913 sampling pixels, were used to define 10 spectral classes. A supervised classification of the subimage was done with this information from the training fields (Table 3 and Fig. 4).

In the above classification, less than 19% were unclassified pixels, so the remaining percentage (81%) was classified, considering the whole subscene. In order to determine the ground covering and how well the classification has categorized a representative subset of pixels used in the training process and using the statistics extracted, the classification error matrix was obtained (Lillesand and Kiefer, 1994 p. 613). The error matrix comprised the 7299 classified pixels, 433 in *L. racemosa* mangrove category (L), of which 415 were correctly classified, 14 were omitted, 13 were erroneously classified as *A. germinans* mangrove (Av), and 1 was misclassified as marsh (P) (Table 4). On the other hand, 18 pixels were included in this category, although they belonged to the *A. germinans* mangrove. Similarly, 539 pixels were classified as *A. germinans* mangrove, of which 526 were correctly classified, 18 were omitted, and 13 were incorrectly included.

In general, there were a considerable number of correctly classified pixels. In order to assess the accuracy of the classification produced, the omission and inclusion probabilities were evaluated (Table 5). In the second column, the accuracy of the classification for each covering class (category in first column) is shown. The third column contains the omission probability value, that is, the percentage of pixels sampled as belonging to that class and classified as belonging to another. The next two columns show the percentage of accuracy of the classified pixels, as a measure of an actual representation on

Table 6
Changes in mangrove vegetation cover according to mapping units reported by CETENAL, photointerpretation of aerial photographs, and Landsat TM image processing

CETENAL map (1973b) digitization	ha	Our photointerpretation (photographs 1970)	ha	Our satellite image (1993) classification	ha
Mangrove	2417	Mangrove	1065	Mangrove of: *L. racemosa*; *A. germinans*	724

the ground of such category, and the probability of committing the inclusion error. Thus, the probability of correctly classifying a pixel in the category of *L. racemosa* mangrove or *A. germinans* mangrove is 96.7% (producer's accuracy), and even the percentage probability of sampling to obtain correctly classified pixels for both categories are greater (95.8% and 97.6%, user's accuracy) than that of the total accuracy of all classes (88.5%).

Due to its easy isolation with respect to the other classes, and to its homogeneity, the accuracy of the water class classification (A) was 100%, while the lower percentages were obtained in dune vegetation (D), with 68.4%, and secondary vegetation (V), with 70.8%.

3.3. Discriminant analysis

By means of a discriminant analysis of the 10 spectral classes formed on the basis of the three main bands, and using the original value of the pixels, significant differences were shown to exist among the groups. For the discriminant analysis, 7922 sampling points were used as training fields. The *F*-test statistic of the discriminant analysis ($F = 97{,}910$) shows that the groups were significantly different ($p < 0.0001$) from each other in each of the spectral bands (3, 4 and 5).

In order to determine the contribution of each variable to the explained variance in the discriminant analysis, a canonical correlation analysis was performed. The standardized coefficients of the canonic variables (now discriminant functions) in which band 5 was found to have the greatest contribution (-0.7787) to explain the variance of that first function. Band 4 had the greatest contribution (0.8481) to explain the variance in the second function, and band 3 had the greatest weight (1.0267) on the third discriminant function. The discriminant function 1 accounted for 84% of the variance, function 2 accounting for an additional 15%, and both functions explained 99% of the total variance, considering the 10 spectral classes. The differences among the spectral classes were significant ($P < 0.001$), and this supports that the groups of spectral classes, distinguished in the color composite 5/4/3 show 10 classes of vegetation and different land uses, according to their spectral response. Fig. 5 shows the cloud formed by the 7922 sampled points, and within it, the 10 spectral classes were delineated according to the two first discriminants, which explains 99% of the variance. In the same figure, the centroids of the spectral classes can be seen for the first two discriminant functions.

It is assumed that the values of the sampled data for each class, once the model is applied, have a normal distribution, variance homogeneity and independence of errors.

3.4. Changes in mangrove covering

The mangrove vegetation area reported by CETENAL (1973b) in its land use/cover map, considering the same area used for the analysis of the image, resulted to be overestimated in 56% regarding the value obtained in our photointerpretation (1065 ha; Table 6). From the latter mangrove area the current cover is 724 ha, which represents a decrease of 32% in a 23-yr period.

Something similar occurs with the tropical dry forest. Nevertheless, it is likely that the covering classes delineated by CETENAL may have been incorrect. This is confirmed from our photointerpretation' that was done delimiting exclusively the mangrove areas.

4. Discussion

Mangrove of the Santiago River Mouth is a vegetation corridor that links two large areas, the first one is Marismas Nacionales (to the north) and the second one is San Blas (to the south). That mangrove has a vegetation structure very much like that of Marismas Nacionales. According to the data reported by Pool et al. (1977), *R. mangle* is an uncommon species with an average basal area of 1.6 m^2 ha^{-1} and an average density of 465 trees ha^{-1}, *L. racemosa* has an average basal area of 37.5 m^2 ha^{-1} and an average density of 1041 trees ha^{-1}, and *A. germinans* has an average basal area of 7 m^2 ha^{-1} and an average density 977 trees ha^{-1}, due to this fact, the first one *L. racemosa* predominates with a higher importance value of 67%, followed by *A. germinans* with a value of 60%, and *R. mangle* with a value of

23%. There are dominance conditions and/or importance values that change in favor of *R. mangle* toward the south, that is toward the mangroves of San Blas Bay (Nayarit) and Barra de Navidad (Jalisco) (Flores-Verdugo et al., 1992). Nevertheless, the mangrove of our study area is dominated by *L. racemosa* with the average importance value of 158.18 and 400 ha of plant cover, followed by *A. germinans*, with an average importance value of 138.52 and 324 ha of plant cover.

Similarly to the lagoonal system of Marismas Nacionales, where the basin acts as a reservoir rich in nutrients (Flores-Verdugo et al., 1992), the Santiago River Mouth mangrove established in the alluvial plain is subject to sediment inputs from the Santiago River, and to the hydric and sedimentary exchange due to tides. The Santiago River Mouth mangrove, nevertheless, presents small values of basal area when compared with those of Marismas Nacionales, though the structure and dominance in the floristic composition are similar.

A good spectral classification was achieved for the mangrove vegetation, due to the identification of the plant associations, which resulted from the compass line and a better visual identification on the ground, as well as using the aerial video obtained, which lead to a better selection of training fields using the false color composite of subscene. The validation of image processing results has been established from the information obtained in the field and that observed in the aerial video and, through photointerpretation. The latter was exclusive of those information classes which interested us the most, that is, the areas classified as mangroves, which presented either one of the dominant species, and had a visual evaluation of the classification obtained in the mangrove community by comparing the classified pixels with the structural data obtained in the field. This certifies that the classification was properly performed in grouping the species associations.

For several information classes, there is almost complete certainty that the classified areas correspond to reality, such as water, dune, marsh, secondary vegetation and sand. It is impossible to assert that the established classification of the other classes corresponds exactly with the grouped areas, for example, in the case of farming areas, grazing areas, fallow fields, salt pits, etc.

In this research, we applied both the discriminant and the canonical-correlation analysis to outline the ten spectral classes that were significantly different (among the groups) and to determine the contribution of each variable to the explained variance in the previous discriminant analysis. This represents an original approach where such a combination of methods has been used. Leading us thereby, to produce the land use/cover map of the study area. The contribution made by each class in each band to the explained variance was also determined, in order to insure that the vegetation associations delineated by means of the image classification results correspond to the 'real' vegetation (type and extent) of the study area.

Considering that we have determined that mangrove area is composed by the dominant association of *L. racemosa–A. germinans* alone, without tropical dry forest components, one of main contribution of this research was that we found an overestimation in the extent of mangrove by CETENAL, in their land use/cover map (1973b). They classified a larger area as mangrove, including a tropical dry forest community too, which is clearly determinable in the 1970 aerial photographs. This wrong classification by CETENAL is possible to demonstrate by the fact that the alluvial plain, where mangrove grows, is subjected constantly to flood periods, which constitutes an unfavorable habitat for the development of tropical dry forest trees.

It is important to highlight the increase of grazing areas, which in aerial photographs of 1970 occupied little more than 650 ha, compared with the more than 2000 ha estimated by the current image analysis. This indicates that the grazing activity increased in 300% in the study area, having as consequence the shrinkage of the primary community of mangrove and tropical dry forest.

Ortíz-Pérez and Romo-Aguilar (1994) evaluated the trajectory changes of the Santiago River from a morphometric and morphographic approach of areas where more evidence is shown (areas with meandering patterns), and from their photointerpretation and considering LandsatTM imagery too, from 1945 to 1993. After comparing the changes with the river path digitized, using both the CETENAL (1973a) and the processed subscene in this work (April 1993), we conclude that no effect was found of significant

modification of the area of mangrove cover, since the dynamics of path changes have been found mainly in areas outside such community (Fig. 6).

With the supervised classification, it was possible to separate, in a representative way, the spectral classes that correspond to the mangrove dominated

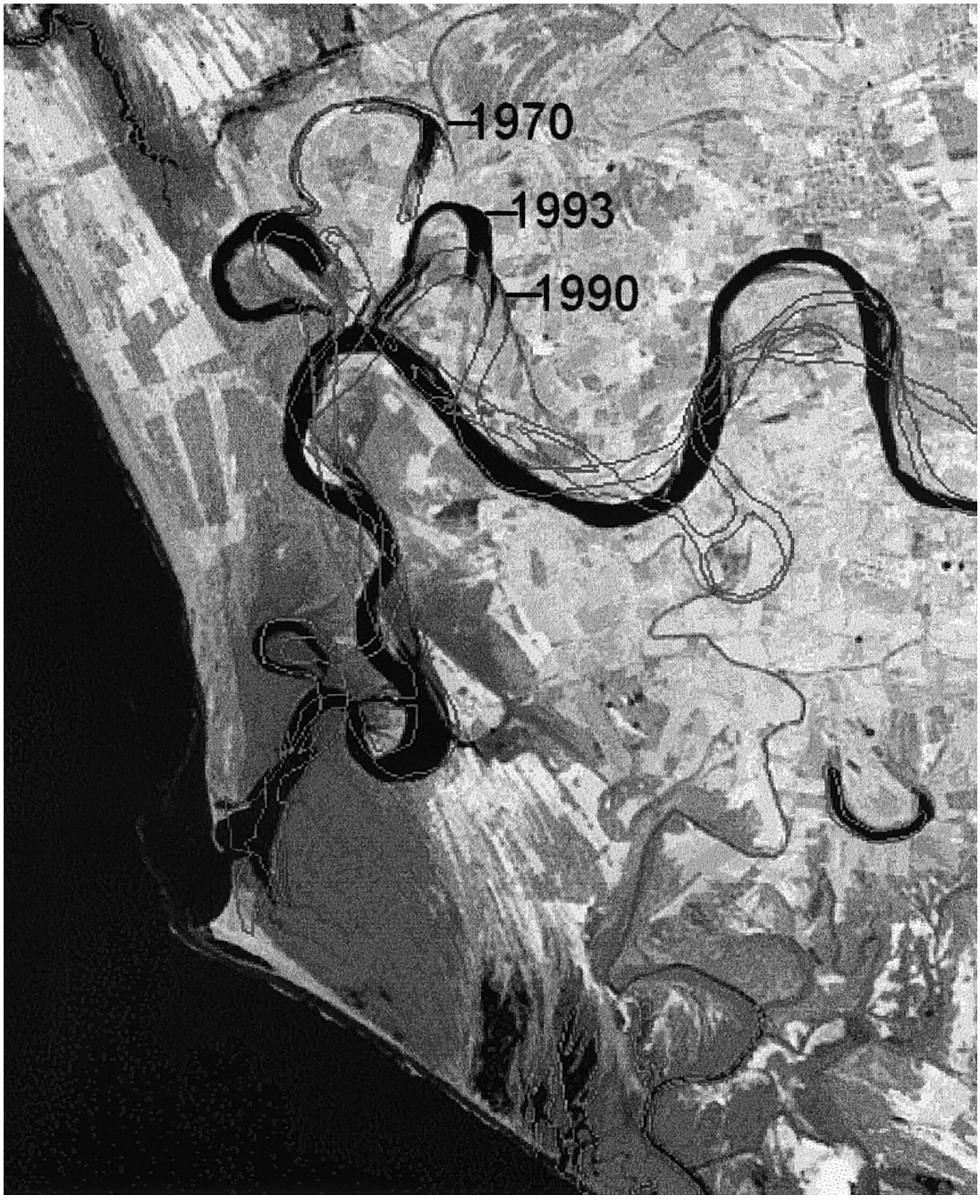

Fig. 6.

by *L. racemosa* and to the one dominated by *A. germinans*. It was also possible to distinguish the farming of induced grazing from the remnants of tropical dry forest found in the study area.

It is evident that the area has experienced substantial deforestation, slightly greater than 30% for the mangrove, as a consequence of an increase of the area occupied for cattle raising. The increase in the area of induced grazing and the direct use for wood exploitation by the tobacco industry (pers. commun. of villagers) have caused a considerable decrease in the area and distribution of mangrove community in the last decades.

Supposing that the change rate of mangrove vegetation cover in our study area has been constant during the 23-yr period considered, the estimated annual rate is 1.4%. Saenger et al. (1983) reported a loss of 130,000 to 155,000 ha of the Indian mangrove forest, in the last 100 years. This could represent an annual rate of 0.4 to 0.6% (considering the mangrove area extent reported by Blasco et al., 1992), if a constant rate of cover change is maintained. However, it is quite possible that this change rate in India could have increased in the last 30 years. Blasco et al. (1992), for example, reported a 70% of mangrove loss in the Philippines over the last 70 years. Under the assumption of a constant rate, this represents an annual change of 1%.

Although the above mentioned percentages are only estimations, they allow us to conclude that the change rate of vegetation cover, due to deforestation, in our study area, is alarmingly high. Furthermore, we have to consider that the largest mangrove forest corridor of Mexican Pacific Coast is in danger, and has been recently ruptured (divided) beginning in a small area between Marismas Nacionales and San Blas (our study area, see Figs. 4 and 6). In the present study, we have to emphasize that fact, and in convenient conditions will allow us, in the near future, to propose the application of ecological restoration measures based on detailed, reliable field information, leading to the mangrove vegetation regrowth in that part of Mexico.

Additional pressures are threatening this mangrove, such as the development of dams built upstream (the Aguamilpa hydroelectric plant). Constant monitoring of the conditions of the Santiago River Mouth mangrove, as well as an efficient management of the hydraulic discharge in such a way that the natural waterflow of the alluvial plain where this mangrove is located is not curtailed, are needed to ensure maintenance of this important mangrove area.

Acknowledgements

The present work was commissioned and financed by the Federal Commission of Electricity and was supported by the Institute of Biology, UNAM, for its fulfilment. We thank M.Sc. Marta Olvera G. and Biologist Carmen Ramírez A. for their participation in the field work, and Dr. Carlos Duarte, Dr. Jorge Meave and Dr. Fernando Chiang for their comments to the manuscript.

References

Blasco, F., 1988a. The international vegetation map (Toulouse, France). In: Kuchler, A.W., Zonneveld, I.S. (Eds.), Vegetation Mapping. Junk Publishers, Amsterdam, pp. 443–460.

Blasco, F., 1988b. Estudio sobre los manglares y la vegetación tropical utilizando datos proporcionados por satélites. Institute de la Carte Internationale de la Végétation. Inst. Inter. Map Vegetat., Univ. Paul Sabatier. Toulouse.

Blasco, F., 1991. Los manglares. [The mangroves] Mundo Científico 11 (114), 616–625.

Blasco, F., France, B.M., Chaudhury, M.U., 1992. Estimating the extent of floods in Bangladesh using SPOT data. Remote Sens. Environ. 39, 167–178.

Chapman, V.J., 1969. Lagoons and Mangrove Vegetation. In: Ayala-Castañares, A., Phleger, F.B. (Eds.). Lagunas Costeras, un simposio. UNAM-UNESCO, No. 28-30, México, pp. 504–514.

CETENAL, 1973a. Topographic Map (sheet Villa Juárez, key F-13-C-28, scale 1:50,000). Comisión de Estudios del Territorio Nacional, México.

CETENAL, 1973b. Land Use/Cover Map (sheet Villa Juárez, key F-13-C-28, scale 1:50,000). Comisión de Estudios del Territorio Nacional, México.

Cintrón, G., Scheaffer, Y., 1984. Methods for Studying Mangrove Structure. In: Snedaker, S.C., Snedaker, J.G. (Eds.), The Mangrove Ecosystem: Research Methods. UNESCO, Bungay, UK, pp. 91–113.

Cox, W.G., 1967. Laboratory Manual of General Ecology, 1st edn. Brown, IA.

Everitt, J.H., Judd, F.W., 1989. Using remote sensing techniques to distinguish and monitor Black Mangrove (*Avicennia germinans*). J. Coastal Res. 5 (4), 737–745.

Everitt, J.H., Escobar, D.E., Judd, F.W., 1991. Evaluation of airborne video imagery for distinguishing Black Mangrove (*Avicennia germinans*) on the lower Texas Gulf Coast. J. Coastal Res. 7 (4), 1169–1173.

Ferrusquía-Villafranca, I., 1993. Geology of Mexico: A Synopsis. In: Ramamoorthy, T.P., Bye, R., Lot, A., Fa, J. (Eds.), Biological Diversity of Mexico: Origins and Distribution. Oxford Univ. Press, Oxford, pp. 3–108.

Flores-Verdugo, F., González-Farías, F., Zamorano, D.S., Ramírez-García, P., 1992. Mangrove Ecosystems of the Pacific Coast of Mexico: Distribution, Structure, Litterfall, and Detritus Dynamics. In: Seeliger, E. (Ed.), Coastal Plant Communities of Latin America. Academic Press, New York, pp. 269–288.

Galavís, S.A., Gutiérrez, E.M.A., 1989. Rasgos morfológicos costeros y litorales de Nayarit y Norte de Jalisco, México. In: Alvarez, R. (Ed.), Tercer Simposio Latinoamericano sobre Sensores Remotos. Sociedad de Especialistas Latinoamericanos en Percepción Remota e Instituto de Geografía, UNAM, México, pp. 116–125.

García, E., 1988. Modificaciones al Sistema de Clasificación Climática de Köppen, 1st edn. Enriqueta García de Miranda, Mexico, 75–203 p.

ITC, 1993. ILWIS The Integrated Land and Water Information System, User's Manual. International Institute for Aerospace Survey and Earth Sciences, Enschede, Netherlands.

Lanza de Izla, G., Ramírez-García, P., Thomas, Y.-F., Alcántara, A.R., 1993. La vegetación de manglar en la laguna de Términos, Campeche. Evaluación preliminar a través de imágenes LANDSAT. [The mangrove vegetation in the Terminos Lagoon, Campeche. A preliminary assessment by means of Landsat imagery] Hidrobiológica 3 (1-2), 30–39.

Lillesand, T.M., Kiefer, R.W., 1994. Remote Sensing and Image Interpretation, 3rd edn. Wiley, New York, pp. 585–618.

Lot, A., Novelo, A., 1990. Forested Wetlands of Mexico. In: Lugo, A.E., Brison, M., Brown, S. (Eds.), Ecosystems of The World 15, Forested Wetlands. Elsevier, Amsterdam, pp. 287–298.

Lugo, A.E., Snedaker, S.C., 1974. The ecology of mangroves. Annu. Rev. Ecol. Syst. 5, 39–64.

Mueller-Dombois, D., Ellenberg, H., 1974. Aims and Methods of Vegetation Ecology, 1st edn. Wiley, New York.

Ortíz-Pérez, M.A., Romo-Aguilar, M.L., 1994. Modificaciones de la trayectoria meándrica en el curso bajo del Río Grande de Santiago, Nayarit, México. [Changes of meander trajectories of the Santiago River downstream Nayarit, Mexico] Bol. Invest. Geogr. 29, 9–23.

Pool, D.J., Snedaker, S.C., Lugo, A.E., 1977. Structure of mangrove forests in Florida, Puerto Rico, Mexico, and Costa Rica. Biotropica 9 (3), 195–212.

Rollet, B., 1974a. Introduction a l'Etude des Mangroves du Mexique: Part I.[An introduction to the study of Mexican mangroves: Part I.] Rev. Bois Forets Tropiques 156, 3–26.

Rollet, B., 1974b. Introduction a l'Etude des Mangroves du Mexique: Part II.[An introduction to the study of Mexican Mangroves: Part 2.] Rev. Bois Forets Tropiques 157, 53–74.

Rollet, B., 1974c. Ecología y reforestación de los manglares de México. ONU/FAO, FI:SF/MEX, p. 15.

Saenger, P., Hegerl, E.J., Davie, J.D.S., 1983. The causes and consequences of mangrove destruction (Global status of mangrove ecosystems). Environmentalist 3 (Suppl. 3), S33–S50.

Secretaría de Recursos Hidráulicos, 1965. Cuenca del Rio Santiago desde la cortina de Poncitiá hasta su desembocadura en el Océano Pacifico. [The Santiago River Basin from the Poncitian Dam to its mouth in the Pacific Ocean] Bol. Hidrol. 25, 1–402.

Sturges, N.A., 1926. The choice of class interval. J. Am. Statistical Assoc. 21, 65–66.